



Published in final edited form as:

Macromolecules. 2009 May 12; 42(9): 3391–3398. doi:10.1021/ma801966r.

Polybasic Nanomatrices Prepared By UV-initiated Photopolymerization

Omar Z. Fisher[†] and Nicholas A. Peppas^{†,‡,¥,*}

[†]Department of Biomedical Engineering, University of Texas at Austin, 1 University Station C0400, Austin, TX 78712-1062 USA

[‡]Department of Chemical Engineering, University of Texas at Austin, 1 University Station C0400, Austin, TX 78712-1062 USA

[¥]Division of Pharmaceutics, University of Texas at Austin, 1 University Station C0400, Austin, TX 78712-1062 USA

Abstract

A novel method for synthesizing nanoscale polymer networks that swell in acidic media is described here using photoinitiated emulsion polymerization. These nanomatrices consist of a crosslinked core of poly[2-(diethylamino)ethyl methacrylate] surface grafted with poly(ethylene glycol) (PDGP) with an average diameter of 50-150 nm. Control over mesh size, surface charge, encapsulation efficiency and in vitro biocompatibility was obtained by varying crosslinking density. The ability to image nanomatrices in their dry state using conventional scanning electron microscopy was made possible by increasing crosslinking density. Theoretical calculations of matrix mesh sizes were supported by the encapsulation of both insulin and colloidal gold 2-5 nm in diameter. The ability to sequester and control the aggregation of an inorganic phase confirmed their use as a nanocomposite matrix material. These networks could be used as imaging agents, drug delivery devices or as components of sensing devices.

Keywords

Hydrogel; Emulsions; pH-responsive; Nanomatrix; Photopolymerization

1. Introduction

Nanogels that exhibit aqueous swelling below a critical pH have many potential applications as nanoactuators, drug delivery devices and sensing agents. Yet, they have received much lower attention than similar, self-assembled nanostructures. The advantage of crosslinking is enhanced structural integrity and control over swelling and transport properties. Here the emulsion polymerization of pH-responsive, polybasic nanoscale matrices using photopolymerization is described. The responsiveness is caused by the presence of weakly basic pendant groups that ionize at or below physiological pH. These networks can be tailored to encapsulate, deliver or sequester specific therapeutic or diagnostic agents.

Gene delivery has been a widely investigated application for nanostructures based on weakly basic polyamines. Many of these polymers are amphiphilic and partially cationized at physiological pH. The presence of protonated amines along the polymer chain allows them to

*To whom correspondence should be addressed. Email: peppas@che.utexas.edu, Tel: 512 471 6644, Fax: 512 471 8227

self-assemble into nanoparticulate polyelectrolyte complexes with polyanions, such as nucleotides. This electrostatic attraction can also be used to bind monoanions. For example, Renagel® (sevelamer hydrochloride) and Renvela® (sevelamer carbonate) are two clinically available polyamines that sequester phosphate ions for the treatment of chronic kidney disease. Likewise, these structures also bind to negatively charged groups on cell surfaces.^{1, 2} This explains their ability to gain entry into the cell, but it is also the reason for their significant toxicity.

The monomer 2-(diethylamino)ethyl methacrylate (DEAEM) is a tertiary amine containing methacrylate that can undergo free radical polymerizations. It has previously been used to synthesize homopolymers and various copolymers, both in its native and ammonium salt form. The resulting homopolymer, poly[2-(diethylamino)ethyl methacrylate] (PDEAEM), undergoes a pH-dependent phase change between hydrophobe and hydrophile.

PDEAEM precipitates out of aqueous solution at a pH above its pK_a and forms into a soft, tacky substance with a T_g below ambient temperature.³ Shatkay and Michaeli⁴ first described the buffering range of PDEAEM with respect to its pH-dependent phase transition. They determined that phase separation occurs at pH values just below the polymer pK_a . They observed a precipitation point at 7.48, and determined a pK_a of 7.68 by titration. Other groups have reported pK_a 's between 7.0-7.3.⁵ Siegel and Cornejo-Bravo^{3, 6} investigated the buffering properties of PDEAEM and its relationship to hydrophobicity. They showed that the polymer pK_a and water sorption decreases when DEAEM is copolymerized along with more hydrophobic monomers.

Schwarte and Peppas^{7, 8} used DEAEM in the fabrication of copolymer networks that display pH triggered swelling. The mesh sizes of these networks could be controlled by varying comonomer feed and crosslinking ratios. These changes were verified by measuring the diffusion of large and small molecular weight solutes through the networks. These studies demonstrated the feasibility of PDEAEM networks as controlled drug delivery agents. However, the hydrophobicity of the networks above the critical swelling pH was compromised by introducing hydrophilic poly(ethylene glycol) (PEG) chains. Both Kost and Goldraich⁹, and Hariharan and Peppas¹⁰ used 2-hydroxyethyl methacrylate as a comonomer and attained similar results. Increasing the hydrophilicity of PDEAEM by copolymerizing with more hydrophilic monomers increases the network pK_a . These earlier studies were done using solution polymerization. A heterogeneous polymerization could take advantage of the hydrophobicity of DEAEM to obtain surface hydrophilicity while maintaining a separate, hydrophobic phase.

Another advantage of heterogeneous polymerization is that increased surface area can provide faster responsiveness. Podual and coworkers exploited the responsive properties of PEG grafted PDEAEM networks to make glucose responsive networks.¹¹⁻¹⁴ They showed that P (DEAEM-g-PEG) microgels, prepared in suspension, had a faster response to changes in pH than larger sized gels.¹² The size of PDEAEM-based networks was further reduced to the nanoscale using thermally initiated emulsion polymerization.^{5, 15, 16} This method achieved nanomatrices from 50-700 nm that were charge and/or sterically stabilized in water. However, the synthesis required reaction times ≥ 24 hr. A photoinitiated method could provide faster initiation and a much shorter reaction time.

Depending on the synthesis method, the buffering range of PDEAEM is either just above or slightly below the physiological pH of 7.4. A pK_a slightly below this would be ideal for most biomedical applications. For example, as an intracellular delivery agent a slight drop in pH would trigger the network to swell.¹⁷⁻¹⁹ Copolymerizing DEAEM with more hydrophilic comonomers such as PEG increases the network pK_a by reducing the proton activity needed

for ionization.⁶ Emulsion polymerization can allow PEG to be surface grafted onto PDEAEM networks, but not interfere with the buffering properties. The resulting system would also be water dispersible at all pH values.

The effect of crosslinking density on the nanoscale material properties of PDEAEM networks has not been fully determined. Because of the large surface area per mass of nanomaterials, they can swell to equilibrium much faster than larger systems. Enhanced crosslinking may not affect swelling as it would for larger systems. In this work the relationship between crosslinking density and network properties is investigated. Also, a novel synthesis strategy was developed to create pegylated PDEAEM nanomaterials more efficiently. The network morphology and cytocompatibility of these structures were studied to elucidate their potential as drug delivery agents.

2. Experimental Section

2.1 Materials

The chemicals 2-(diethylamino)ethyl methacrylate, Brij-30, Brij-35, bovine insulin, myristyltrimethylammonium bromide (MyTAB), poly(ethylene glycol) monomethyl ether monomethacrylate ($M_n=2080$, 50wt% aqueous solution) (PEGMMA), sodium dodecyl sulfate (SDS), tetrachloroauric(III) acid, tetraethylene glycol dimethacrylate (TEGDMA), and tetrakis (hydroxymethyl)phosphonium chloride (THPC) were all obtained from Sigma-Aldrich Corporation. Deuterium chloride (DCl; 20% in D_2O), hydrochloric acid 1N solution (HCl), Pluronic F-68 and sodium hydroxide 1N solution (NaOH) were obtained from Thermo-Fisher Scientific. Irgacure 2959 was obtained from Ciba Chemical Company. Dulbecco's Modified Eagles Media (DMEM) and NIH/3T3 mouse fibroblasts were obtained from American Type Culture Collection (ATCC, Manassas, VA). Bovine calf serum and 10x phosphate buffered saline (PBS) were obtained from Mediatech Inc. Deuterium oxide (D_2O) was obtained from Cambridge Isotope Laboratories Inc. (Andover, MA).

2.2 Photo-emulsion Polymerization

PDGP nanomaterials were polymerized by emulsion polymerization as described: All monomers were passed through a column of basic alumina powder to remove inhibitor prior to use. In a glass beaker, a mixture TEGDMA, and DEAEM was added to a 50 mL aqueous solution of 5 wt% PEGMMA, Irgacure 2959 at 0.5 wt% of total monomer, and various surfactants in deionized distilled water (ddH_2O). A range of surfactant mixtures were evaluated to determine which was best suited for maintaining emulsion stability, and which would achieve the smallest nanogel size. Emulsion stability was checked by placing a drop of the emulsion between a glass slide and coverslip and viewing it at 40x objective magnification. If the coalescence of fat droplets could be viewed then the emulsion was deemed unstable. TEGDMA was used at X values of 0.01, 0.025, 0.05, 0.10 and 0.20, where X is the crosslinking mole feed ratio. The DEAEM content was kept constant at 5 wt% monomer in water.

The mixture was emulsified for 10 minutes using a Misonix Ultrasonicator (Misonix Inc., Farmingdale, NY) at 88 W while partially submerged in a stirred ice water bath. The emulsion was then purged with nitrogen gas for ten minutes, capped, then exposed to a UV point source for 2 hr at 140 mW/cm^2 with the light guide directed at the top of the emulsion, all with constant stirring. PDEAEM homopolymer and crosslinked networks were prepared using the same synthesis conditions without PEGMMA and TEGDMA, or just without PEGMMA. PDGP graft copolymer was prepared using the same conditions but without crosslinking.

The removal of unreacted reagents and surfactants was performed by collapsing, aggregating and centrifuging the suspended particles in their cationized state. First, an equal volume 1 N

HCL was added to the suspension to fully protonate the particles. Acetone was then added to the suspension up to a final concentration of 70%, the point at which the particles flocculated and began to sediment. The mixture was then centrifuged at 3200 g for 10 minutes to fully separate out the precipitate. The solvent was then poured off and the pellet was resuspended again in 0.5 N HCl. The precipitation/centrifugation/resuspension steps were repeated 5 times with a final resuspension in water. The suspensions were then dialyzed (MWCO=15kDa) for 5 days, with water being replaced twice daily, until the pH of the supernatant matched the pH of water. The suspension was then flash frozen in liquid nitrogen, lyophilized, and finally placed in a vacuum oven at 30° C until further use. Polymers prepared without crosslinker were precipitated similarly but centrifuged at 33,000 g.

3. Results and Discussion

3.1 Photo-emulsion Polymerization

A successful emulsion polymerization scheme for the synthesis of PEG surface-grafted poly [2-(diethylamino)ethyl methacrylate] (PDGP) nanomatrices was determined empirically and qualitatively. The goal was to attain nanomatrices that behaved as shown in Figure 1, where a transition between collapsed gel, polyelectrolyte gel, and ionomer gel is shown. These states were exploited for processing and loading.

In oil-in-water emulsion polymerization the self-assembly of surfactants into micelles is required. Although a two phase system is established, polymerization begins not in the water or monomer droplet phase but in the micellar phase. For this reason the concentration of surfactants used must be above the critical micellar concentration (CMC). Growing nanoparticles are continuously fed monomer and free radicals from the surrounding water phase. The rate of polymerization can be increased by reducing the size of the monomer droplets.²⁰

In this work monomer droplet size was checked using optical microscopy. Droplet size was influenced by mechanical agitation, choice and concentration of surfactant. When initially compared, ultrasonication for ten minutes resulted in smaller droplet sizes than ultrahomogenization at 24,000 rpm. The size distribution also appeared to be narrower when ultrasonication was used. Sonication was used for all further investigations. The emulsion was established using ultrasonication and maintained throughout the polymerization by mechanical stirring. This is in contrast to other schemes where mechanical stirring is used both to create and maintain the emulsion throughout the reaction. This required that the emulsion remain stable after sonication.

The ionic surfactants, myristyltrimethylammonium bromide (MyTAB) and sodium dodecyl sulfate (SDS), were both able to establish and maintain macro- and microemulsions at concentrations ranging from 0.5-3x the critical micellar concentration (CMC). However, microemulsions did not produce detectable particles. SDS was used first, as a proof of concept, because of its success in previous work.⁵ The cationic surfactant MyTAB was chosen as a replacement to eliminate the possibility of electrostatic attraction between the surfactant and the particles during the surfactant removal process. When used alone, none of the nonionic surfactants were able to sustain microemulsions at any concentration. When Pluronic F-68 at 0.2-2 wt% was used, the result was acid swellable microgels with diameters in the 0.8-50 μm range. These contained large internal cavities that were only visible when the gels were swollen (Figure 2A). These could have been the result of incomplete suspension polymerization or a pseudo-w/o/w emulsion. The evacuation of these large cavities under vacuum may have resulted in the pores seen using scanning electron microscopy (Figure 2B). The use of Brij-35 and Triton X-100 achieved similar results. Using SDS below the CMC achieved microgels 0.8-1 μm in diameter (Figure 2C).

A mixture of 3.4 mM MyTAB with any nonionic cosurfactants was successful in maintaining emulsion stability. However, MyTAB with 2 mg/ml Brij-30 was the only surfactant mixture that resulted in particle diameters well below 1 μm . The polydispersity and average particle size were also dependent on the concentration of Brij-30. Both of these were lowered when the concentration of Brij-30 was increased to 4 mg/mL. Using Brij-30 alone was unable to maintain emulsion stability. Brij-30 is distinct from the other nonionic surfactants used because of its low hydrophile-lipophile balance ratio (HLB). A nonionic surfactant with an HLB ratio of ≥ 10 is typically used for an oil-in-water emulsion. Those with an HLB ratio of < 10 are typically used for inverse emulsions. The HLB ratio for Brij-30 is 9.7. The HLB ratios for Triton X-100, Pluronic F-68 and Brij-35 are 13.5, 24 and 16.9, respectively as provided by the manufacturers.

According to previous work, a minimum PEG graft size of 2 kDa is needed to minimize non-specific protein adsorption.²¹ The use of molecular weights that were higher than 5000 was shown to be less efficient. This is likely due to their tendency to form tighter coils. In this work a length of 2000 was chosen for preliminary work. Amalvy and coworkers⁵ were able to use methacrylated PEG grafts alone, both as steric stabilizer and emulsifier, in the thermoinitiated emulsion polymerization of nanomatrices. The use of poly(ethylene glycol) monomethyl ether monomethacrylate (PEGMMA) (MW=2080) alone in our work was insufficient in maintaining emulsion stability yet when removed from the reaction, there was visible flocculation after reacting for 1 hr. To confirm that PEGMMA was acting as a steric stabilizer, it was replaced with PEG monomethyl ether (MW=1900) in one reaction. This suspension also flocculated and settled to the bottom of the flask after 1 hr. Polymer networks could be obtained in as little as 15 minutes. But a reaction time of at least 2 hours was needed to obtain nanomatrices that did not flocculate in water above a pH of 7.3. This provided an observable way to check for the presence of PEG grafts on the surface. These observations were later confirmed by NMR.

The removal of surfactant and unreacted monomer from nanomatrices was achieved by inducing a polyelectrolyte-to-ionomer transition.²² The chloride salt form of the tertiary amine is present when PDGP is suspended in water containing sufficient hydrochloric acid. The network can be collapsed while keeping the pendant groups ionized by lowering the dielectric constant of the suspension (Figure 1). This could be done by adding a weak organic solvent. When 70% acetone was added to nanomatrices suspended in 0.5N hydrochloric acid (HCL), the transition from swollen gel to collapsed ionomer was achieved. This caused immediate flocculation and sedimentation of the particles. The ionomer phase was then isolated by centrifugation. The pellet could then be resuspended in water and the process repeated. The unreacted monomers and surfactants were checked and found to be all soluble in 70% acetone in 0.5 N HCL. After a final resuspension in water, the excess hydrochloric acid could be washed out by dialysis. Uncrosslinked PDEAEM and PDGP would precipitate into a suspension that could be separated from the solvent, but only by using a much higher centrifugal force than for networks.

3.2 ^1H NMR Analysis

The ^1H NMR spectra for PDGP showed the additional presence of the oxyethylene peak from PEG grafts when compared to the spectra for PDEAEM, confirming pegylation (Figure 3). The absence of the oxyethylene peak in the PDEAEM sample also confirmed the removal of Brij-30. The amount of comonomer incorporated onto the network was quantified by comparing the ratio of peak area for the methylamine peak at 3.2 ppm to that of the oxyethylene peak area at 3.6 ppm. Specifically,

$$1H\text{ratio} = \frac{A_{PEG} - A_{B,PEG}}{A_{meth} - A_{B,meth}} \quad (1)$$

where A_{PEG} is the peak area of the oxyethylene group, $A_{B,PEG}$ is the area of background with the same ppm spread, A_{meth} is the peak area for the methylamine, and $A_{B,meth}$ is the area of background with the same ppm spread as the methylamine. The comonomer ratio could be calculated from the proton ratio by using the number of protons on each pendant group. For PDGP the DEAEM/PEGMMA ratio was 226, or 4.7 wt% PEG. The spectrum for the pegylated compound matches that published by Amalvy and coworkers.⁵ for a lightly crosslinked microgel. When NMR spectra were measured for crosslinked particles, signal attenuation was significant and increased with the crosslinking feed. Also, as the crosslinking feed increased, the oxyethylene peak area increased while all other peak areas decreased, relative to the background. While this effect confirms that the PEG is confined to the surface, analysis of the spectra would result in an overestimate of pegylation.

The practical advantage of keeping the particles in their fully protonated state after processing was that they were more easily handled than deprotonated samples. Deprotonated, dried nanomatrices were soft and tacky. This is consistent with the film forming property of PDEAEM containing micro and nanomatrices observed in other work.⁵ This property also presents a complication for electron microscopy. Because PDGP particles tend to spread on a surface at ambient temperature, it was virtually impossible to observe their morphology using conventional scanning electron microscopy. The same is true for unfixed biological soft tissue. The common solution is to use a crosslinking agent such as gluteraldehyde to enhance the integrity of the sample. We attempted to determine if increased crosslinking had a similar effect of the nanomatrices.

Scanning electron microscopy showed that the ability to discern the size and morphology of nanomatrices was dependent upon ionization and crosslinking density. In general, the ionized salt form of the PDGP networks gave the particles greater integrity under the electron beam. Large, ionized microparticles with 1 mol% feed crosslinking prepared from a Pluronic F-68 emulsion appeared spherical, but typically had pores resulting from the rapid escape of encapsulated solvent (Figure 2B). Replacing Pluronic with SDS resulted in smaller, flattened spheres that tended to dry as monolayers (Figure 2C). Nanomatrices synthesized from a MyTAB/Brij-30 emulsion, with 1 mol% crosslinker in the feed, tended to form semi-coherent films with the vague outline of particles visible in some places (Figure 4A). Crosslinking at 2.5% achieved a similar result. At 5-20% crosslinking the spherical shape of fairly monodisperse protonated nanoparticles became clear (Figure 4B & 4C). For 10% and 20% crosslinked nanomatrices the shape was preserved in both the protonated and deprotonated state.

3.3 Mesh Size

Dynamic light scattering measurements were used to determine the volume of nanomatrices in the swollen state (see Supporting Information for methods). The accuracy of the technique depended on size distribution. The use of Brij-30 below an aqueous concentration of 4 mg/ml resulted in a bimodal distribution of particle sizes. The polydispersity for batches made below this limit was between 0.25-0.4. Also, contrary to expectations, the measured hydrodynamic diameter of these batches decreased as a function of pH (i.e., they responded as if they were polyacidic networks). This was resolved by centrifuging the suspension at 40,000g and thereby separating out the larger particles. This resulted in a suspension with polydispersity consistently <0.100 and the predicted swelling characteristics of a polybasic network. Increasing the Brij-30 concentration during synthesis achieved the same results. The ability to image nanomatrices

at higher crosslinking feed values using electron microscopy was crucial in calculating the volume swelling ratio Q . This value is defined as the ratio of network volume in the swollen state to the volume in the collapsed state. Assuming that each particle formed in the emulsion is a discrete bulk polymerization, the Brannon-Peppas model for polybasic networks with non-Gaussian chain length distributions can be used to determine the molecular weight between crosslinks, \bar{M}_c .^{7, 23, 24}

$$\frac{V_1(\bar{v} Q)^{-2} \left(\frac{K_b}{10^{pH-14} + K_b} \right)^2}{\left(1 - \frac{1}{N} Q^{-\frac{2}{3}} \right)^3} = \frac{\left[\ln \left(1 - \frac{1}{Q} \right) + \frac{1}{Q} + \chi q^{-2} \right] + \left(\frac{V_1}{\bar{v} \bar{M}_c} \right) \left(1 - \frac{2\bar{M}_c}{M_n} \right) \left(Q^{-\frac{1}{3}} - \frac{Q}{2} \right) \left(1 + \frac{1}{N} Q^{-\frac{1}{3}} \right)^2}{\left(1 - \frac{1}{N} Q^{-\frac{2}{3}} \right)^3} \quad (2)$$

Here V_1 is the molar volume of water (18 cm³/mol); I is the ionic strength of the swelling medium, calculated as 1.7 for phosphate buffered saline (PBS); \bar{v} is the specific volume of the polymer, 0.91 g/cm³. K_b is the basic dissociation constant for DEAEM; χ is the Flory polymer-solvent interaction parameter, previously estimated as 0.20¹⁰; \bar{M}_c is the molecular weight of the uncrosslinked polymer, equal to a value of 14,9 kDa as obtained by gel permeation chromatography (GPC) measurements. N is the number of consecutive units between crosslinks, calculated as,

$$N = \frac{\frac{M_n}{M_r}}{\frac{M_n X}{M_r} + 1} \quad (3)$$

Values of the molecular weight between crosslinks and mesh sizes in swollen state are listed for each formulation in Table 1. These experimental values were used to compute a network mesh size. This value is a physical distance between crosslinks and can be used to estimate the upper size limit of agents that can diffuse into and out of the matrix. Assuming an isotropic extension of polymer chains upon swelling, the mesh size can be modeled as,

$$\xi = Q^{\frac{1}{3}} \left[C_n \frac{2\bar{M}_c}{M_r} \right]^{\frac{1}{2}} \ell \quad (4)$$

where C_n is the characteristic ratio for a methacrylate network ($C_n = 11$) and ℓ is the carbon-carbon bond length (0.154 nm). The volume of particles in the dry state was calculated as the cube of the average particle diameter from SEM images. The diameter was measured by drawing lines across a minimum of 30 particles in images taken at each crosslinking feed ratio and scaling them relative to the scale bar. A single average diameter of 50±10 nm was used for all calculations of Q since the measured diameters for crosslinking feed ratios of 0.5, 0.10 and 0.20 were not significantly different.

The estimate for N is based on an idealized, equal distribution of chain junctions, where the uncrosslinked chain is divided into $n + 1$ equally spaced segments and n is equal to the degree of polymerization multiplied by the crosslinking feed ratio (Equation 2). This estimate is not required when using the model for Gaussian chain length distributions, which is applicable for very lightly crosslinked hydrogels.²³ When the mesh sizes obtained using either the model for Gaussian or non-Gaussian chain length distributions were compared the values did not vary much for higher crosslinking values, though they did generally increase when using the Gaussian assumption. For samples with crosslinking feed ratios of 1%, 2.5%, 5% and 10% the

mesh size increased by 5.44 nm, 0.77 nm, 0.37 nm, and 0.3 nm respectively relative to calculations based the assumption of a non-Gaussian chain length distribution was used. The reason for this trend is the relatively small value of M_n and the large influence of crosslinking. Using an artificial value of 1,000 kDa for M_n increased the mesh size for the 1% crosslinked formulation by 5 nm but had negligible impact on samples crosslinked at 2.5%, 5% and 10%. The degree of swelling and mesh sizes for the formulations are plotted as a function of pH in Figure 5. No detectable swelling was measured for samples crosslinked at 20%. The network mesh sizes that were determined reach a maximum just below physiological pH.

Previous attempts to measure volume swelling for submicron particles have relied solely on light scattering data for spatial measurements.⁵ When initial analyses were performed using light scattering measurements at high pH as geometric minimums, the estimated \bar{M}_c and ξ values were unrealistic. Using these values predicted that a particle with a crosslinking feed ratio of 0.025 had a larger degree of swelling than one less crosslinked. These also predicted a maximum mesh size of less than 1.5 nm. This precludes the entrapment of even relatively small macromolecules such as insulin, which has a monomeric radius of 1.3 nm.²⁵

The diameters obtained from light scattering were expected to be slightly higher than in the dry state due to the presence of the surface grafted PEG chains. These were expected to increase the diameter by up to 7 nm based on the Flory radius for a PEG tether with a molecular weight of 2 kDa.²⁶ Yet, the formulation with the lowest crosslinking density had a volume approximately 220% of what would be expected. Despite the hydrophobic nature of the particle core, the larger increase can be accounted for by water absorption. Cornejo-Bravo and Siegel³ investigated the ability of deprotonated, dry PDEAEM to absorb water from the vapor phase. It was determined that this absorption occurred in the form of nucleation around the pendant amines. While not enough to solubilize the polymer, this process did double the dry weight and had a plasticizing effect. Many insoluble natural fibers such as cellulose are plasticized by water in the same way.²⁷

3.4 Insulin Loading

To confirm the ability to macromolecule loading into the network we used insulin as model drug. Loading studies were done over a pH range of 6.5-7.4 (see Supporting Information for methods). HPLC measurements of the nanomatrix supernatant taken at a pH of 6.5 showed that 100% of insulin was uptaken at the two lowest crosslinking densities, $92 \pm 0.3\%$ for a molar feed ratio of 0.05 and $63 \pm 0.7\%$ for a molar feed ratio of 0.10. For all except nanomatrices with a molar feed ratio of 0.01, the values decreased as the pH was raised to 7.4 (Figure 6). Because the loading was performed at a pH above the pI for insulin, the protein was effectively a polyanion, which allowed it to form a polyelectrolyte complex with the polycationic polymer, in the same manner as polyplex formation. This additional electrostatic attraction may make the nanomatrices potentially useful in gene delivery. A network would be more stable than other self assembled carriers such as lipopolyplexes, which are prone to degradation in serum.²⁸ The results showed that the networks could load up to their own weight in a model macromolecule and that loading decreased with decreasing mesh size. The drop in loading as the pH was raised likely resulted from the desorption of surface bound insulin. The loss of charge attraction caused the release of this insulin back into solution.

3.5 Colloidal Gold Loading

Recently there has been significant interest in the design of micro and nanoscale composite inorganic/organic systems. The goal is to combine the advantages of macromolecular chemistry with the unique optical and electrical properties of inorganic nanosystems. For example, colloidal gold, 5-20 nm in diameter, can be trapped into thermoresponsive hydrogel microspheres, making them environmentally responsive imaging agents.²⁹ Though much of

the research on hydrogels in this area has been limited to microgels³⁰, there has also been work to synthesize submicron polymer nanocomposites³¹. Inorganic nanoparticles, such as gold colloids, can be as small as 1 nm in diameter. PDGP nanomatrices theoretically have a network structure that can accommodate particles of this size by simple partitioning. Gold colloids are also known to associate with basic amines, such as the pendant groups on PDGP networks, due to electrostatic attraction.³²⁻³⁵ They also aggregate at pH extremes, resulting in a red shift in their extinction spectrum. Au colloids, 2-5 nm in diameter, do not have a distinct characteristic Plasmon absorption peak in the visible light range.³⁶ But the controlled flocculation of these particles causes the appearance of a peak at 520nm, typical of particles 5-30 nm in diameter. When loaded into PDGP nanomatrices, the network constraints on growth should cause the aggregation of gold nanoparticles to be mesh size limited. To test this we loaded colloidal gold, 2-5 nm in diameter, into the nanomatrices and lowered the pH to induce aggregation (see Supporting Information for methods). The amount of acid added was based on the amount needed to cause a visible color change, from orange-black to blue, in the metal colloid alone. All the samples appeared to support the controlled growth of colloids up to particles 5 nm in diameter (Figure 7). This was confirmed by the presence of an extinction peak at 510 nm for the three lowest crosslinking values and a peak at 520 nm for the highest. The extinction spectra for 1-5% crosslinked samples were identical. But there was noticeable spectral broadening for the sample with the 10% crosslinking density, suggesting the presence of gold nanoparticles larger than 5 nm (Figure 8). Suspensions of nanomatrices alone had no discernable absorbance peak at any wavelength, at the concentrations used.

Transmission electron microscope (TEM) images showed the presence of 2-5 nm gold particles for samples with a crosslinking feed ratio of 0.01 and 0.025 concentrated within flattened, spread particles in a semicoherent film (Figure 7 A & B). This matched the film forming seen with SEM. At 5% crosslinking all the gold colloid was localized within polymer particles, with diameters between 30-70 nm (Figure 7C). Nanogels crosslinked at 10% accommodated gold nanoparticles up to ~5 nm within the polymer networks, but there was also the presence of larger gold particles 10-25 nm associated around the particles (Figure 7D). This suggested that the gold colloid was partly confined to the outside of the nanomatrices, where it was free to form larger aggregates. The polymer networks also appeared to aggregate around the larger gold aggregates. The mesh size calculations predicted that at 10% crosslinking density the network would support little aggregation. This theory fits with the visible exclusion of larger gold particles to the surface of the polymer particle shown in the figure. Confined to the surface, the gold aggregation should eventually overcome the presence of PEG grafts and cause the networks to flocculate.

3.6 Cell Viability

The biocompatibility of PDEAEM-based micro and nanostructures depends on how cationized the pendant amine groups are at physiological pH and how exposed they are to the biological environment. The use of PEG as a steric stabilizer has been shown to increase the in vitro biocompatibility of PDEAEM nanogels¹⁵, yet it is still far below that of similar nanogels³⁷ or polyplexes³⁸. PDGP nanogels show a distinct positive relationship between crosslinking density and cytocompatibility (Figure 9). The IC₅₀ values for nanogels with 1%, 2.5%, and 5% crosslinker monomer feed were 62.5 µg/mL, 125 µg/mL, and 250 µg/mL, respectively. Samples made with 10% crosslinker monomer feed caused no reduction in cell viability at any concentration tested. (see Supporting Information for methods)

Anderson and Mallapragada³⁹ investigated the in vitro cytocompatibility of linear chains of PDEAEM copolymerized with PEG and determined a non-toxic concentration up to 3 µg/mL using NIH/3T3's. Oishi and coworkers¹⁵ also observed a positive relationship between crosslinking density and cytocompatibility for PDEAEM nanogels up 1% crosslinked, but the

authors only compared two different crosslinking ratios. It was postulated that more crosslinking inhibits the free dangling of cationic chain segments, thereby reducing their ability to interact with cell membranes. This is reasonable, given the soft and rubbery nature of the polymer.

The results of this work showed that a change in the buffering range of the system also occurs with increased crosslinking by making the core of the particle more hydrophobic. Siegel and Cornejo-Bravo⁶ demonstrated this effect on linear PDEAEM by copolymerizing with a more hydrophobic comonomer. An increase in the proton energy needed to swell the system would translate into less cationization at a given pH, as predicted by the Henderson-Hasselbalch model⁴⁰. This could also lead to a more biocompatible system.

4. Conclusions

We have successfully used photopolymerization to synthesize polybasic, nanogels capable of encapsulating therapeutic agents that can also serve as scaffolds nanocomposite fabrication. The advantage of using photoinitiation as a driving force was that we achieved a significantly more time efficient reaction than similar emulsion based methods for making PDEAEM based nanogels.^{5, 15, 16} The PEG stabilized nanogels displayed pH-dependent volume swelling with a hydrodynamic diameter between 50-150 nm. By varying crosslinking density we could control the network mesh size and thereby limit the loading of both insulin and gold colloids. This also had the effect of increasing the in vitro biocompatibility of the networks. These have the potential to be used as templates for the controlled growth of other micro and nanostructures, components of sensing and diagnostic devices, or as carriers for the targeted delivery of therapeutic agents.

Supplementary Material

Refer to Web version on PubMed Central for supplementary material.

Acknowledgments

N.A.P. acknowledges support from the National Institutes of Health, grant number EG-000246 and from a National Science Foundation Integrative Graduate Education and Research Traineeship (IGERT) Fellowship (to O.Z.F.), DGE-03-33080. The authors would also like to acknowledge the technical assistance of Helen Lin in the Department of Biomedical Engineering, the resources of the University of Texas at Austin Institute for Cellular and Molecular Biology and the Texas Material Institute.

References

1. Labat-Moleur F, Steffan AM, Brisson C, Perron H, Feugeas O, Furstenberger P, Oberling F, Brambilla E, Behr JP. *Gene Ther* 1996;3:1010. [PubMed: 9044741]
2. Behr JP. *Chimia* 1997;51:34.
3. Cornejo-Bravo JM, Siegel RA. *Biomaterials* 1996;17:1187. [PubMed: 8799503]
4. Shatkay A, Michaeli I. *J Phys Chem* 1966;70:3777.
5. Amalvy JI, Wanless EJ, Li Y, Michailidou V, Armes SP, Duccini Y. *Langmuir* 2004;20:8992. [PubMed: 15461478]
6. Siegel RA, Cornejo-Bravo JM. *ACS Symp Ser* 1992;480:131.
7. Schwarte LM, Peppas NA. *Polymer* 1998;39:6057.
8. Schwarte LM, Peppas NA. *Abstr Pap Am Chem Soc* 1997;214:292.
9. Kost J, Goldraich M. *Abstr Pap Am Chem Soc* 1992;203:113.
10. Hariharan D, Peppas NA. *Polymer* 1996;37:149.
11. Podual K, Doyle F, Peppas NA. *Ind Eng Chem Res* 2004;43:7500.
12. Podual K, Doyle FJ, Peppas NA. *Biomaterials* 2000;21:1439. [PubMed: 10872773]

13. Podual K, Doyle FJ, Peppas NA. *J Control Release* 2000;67:9. [PubMed: 10773324]
14. Podual K, Peppas NA. *Polym Int* 2005;54(3):581–593.
15. Oishi M, Hayashi H, Itaka K, Kataoka K, Nagasaki Y. *Colloid Polym Sci* 2007;285:1055.
16. Hayashi H, Iijima M, Kataoka K, Nagasaki Y. *Macromolecules* 2004;37:5389.
17. Boussif O, Lezoualch F, Zanta MA, Mergny MD, Scherman D, Demeneix B, Behr JP. *Proc Natl Acad Sci U S A* 1995;92:7297. [PubMed: 7638184]
18. Akinc A, Thomas M, Klibanov AM, Langer R. *J Gene Med* 2005;7:657. [PubMed: 15543529]
19. Sonawane ND, Szoka FC, Verkman AS. *J Biol Chem* 2003;278:44826. [PubMed: 12944394]
20. Piirma, I. *Emulsion polymerization*. Academic Press; New York: 1982.
21. Moghimi SM, Hunter AC, Murray JC. *Pharmacol Rev* 2001;53:283. [PubMed: 11356986]
22. Osada, Y.; Khokhlov, AR., editors. *Polymer gels and networks*. Marcel Dekker; New York: 2002.
23. Brannon-Peppas, L.; Harland, RS. *Absorbent polymer technology*. Elsevier Science Pub.; New York, NY, U.S.A.: 1990.
24. Brannon-Peppas L, Peppas NA. *Chem Eng Sci* 1991;46:715.
25. Oliva A, Farina J, Llabres M. *J Chromatogr B Biomed Sci Appl* 2000;749:25. [PubMed: 11129075]
26. Wong JY, Kuhl TL, Israelachvili JN, Mullah N, Zalipsky S. *Science* 1997;275:820. [PubMed: 9012346]
27. Espert A, Vilaplana F, Karlsson S. *Compos Part A Appl Sci Manuf* 2004;35:1267.
28. Li S, Tseng WC, Stolz DB, Wu SP, Watkins SC, Huang L. *Gene Ther* 1999;6:585. [PubMed: 10476218]
29. Kuang M, Wang DY, Mohwald H. *Adv Funct Mater* 2005;15:1611.
30. Pich AZ, Adler HJP. *Polym Int* 2007;56:291.
31. Owens DE, Eby JK, Jian Y, Peppas NA. *J Biomed Mater Res A* 2007;83A:692. [PubMed: 17530631]
32. Oldenburg SJ, Averitt RD, Westcott SL, Halas NJ. *Chem Phys Lett* 1998;288:243.
33. Westcott SL, Oldenburg SJ, Lee TR, Halas NJ. *Langmuir* 1998;14:5396.
34. Averitt RD, Westcott SL, Halas NJ. *J Opt Soc Am B* 1999;16:1824.
35. Nehl CL, Grady NK, Goodrich GP, Tam F, Halas NJ, Hafner JH. *Nano Lett* 2004;4:2355.
36. Duff DG, Baiker A, Edwards PP. *Langmuir* 1993;9:2301.
37. McAllister K, Sazani P, Adam M, Cho MJ, Rubinstein M, Samulski RJ, DeSimone JM. *J Am Chem Soc* 2002;124:15198. [PubMed: 12487595]
38. Funhoff AM, van Nostrum CF, Koning GA, Schuurmans-Nieuwenbroek NM, Crommelin DJ, Hennink WE. *Biomacromolecules* 2004;5:32. [PubMed: 14715005]
39. Anderson BC, Mallapragada SK. *Biomaterials* 2002;23:4345. [PubMed: 12219824]
40. Hasselbalch KA. *Biochem Z* 1916;78:112.

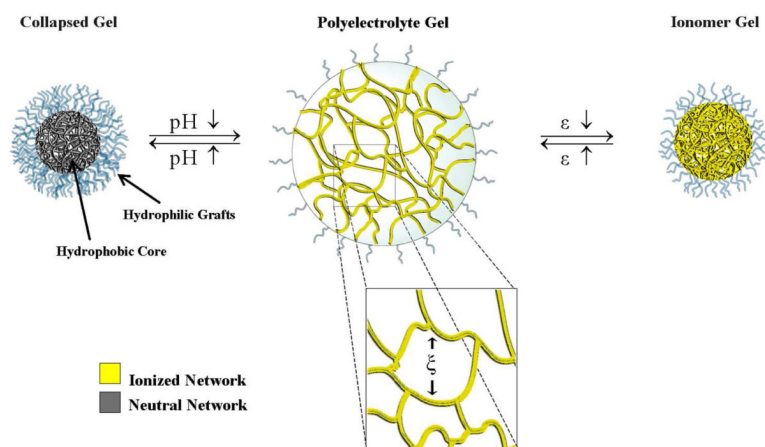


Figure 1.

Environmental Responsiveness - Polybasic nanomatrices will ionize and swell in water at low pH. The influx of water increases the gel mesh size (ξ), allowing additional compounds to be loaded into the matrix. If the dielectric constant of the solvent (ϵ) is reduced, the gel will collapse into an ionomer.

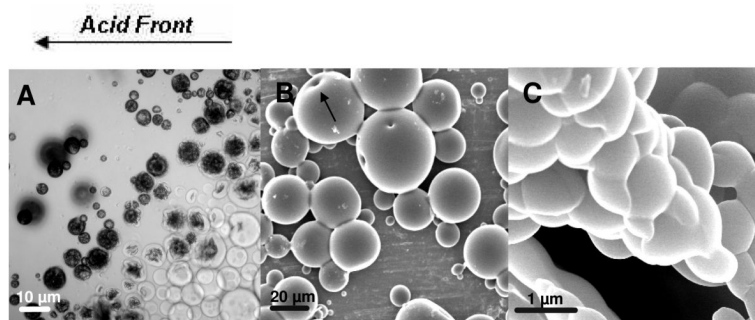


Figure 2. PDGP Microgels. (A) Light microscope image of a microgel suspension, prepared using Pluronic F-68, swelling in an approaching hydrochloric acid front. (B) SEM image of dried PDGP microgels prepared with Pluronic F-68 (B) Microgels prepared from a Pluronic F-68 emulsion. Arrow points to pores that were observed on the surface of larger particles. (C) SEM image of microgels prepared using SDS.

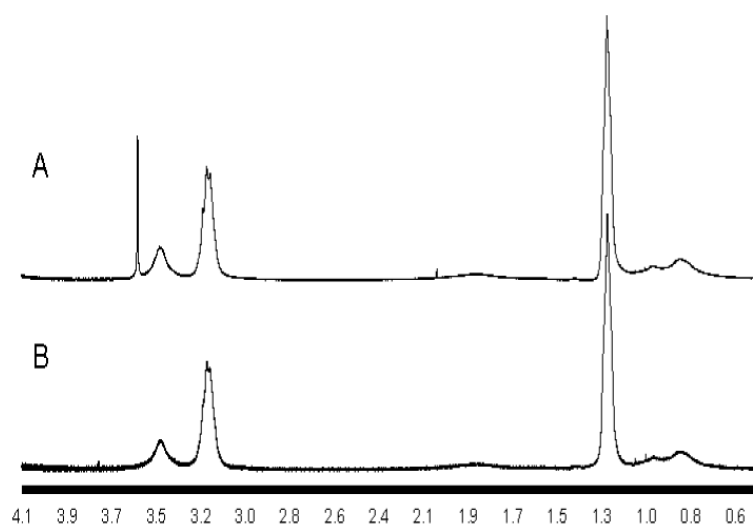


Figure 3. Proton NMR spectra of uncrosslinked PDGP (a) and PDEAEM (b).

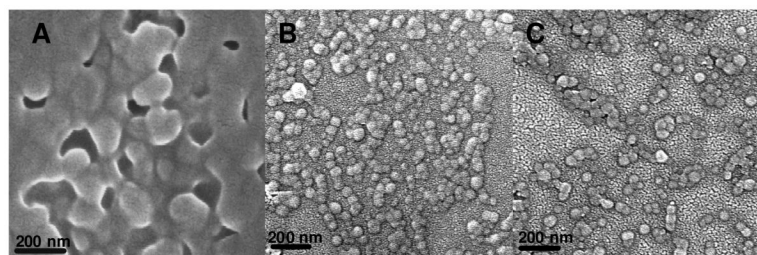


Figure 4. PDGP nanomatrices. (A) Protonated nanomatrices prepared from a MyTAB/Brij-30 emulsion, with 1 mol% crosslinker. (B) Deprotonated nanomatrices prepared from a MyTAB/Brij-30 emulsion, with 5 mol% crosslinker. (C) Protonated nanomatrices prepared from a MyTAB/Brij-30 emulsion with 5 mol% crosslinker.

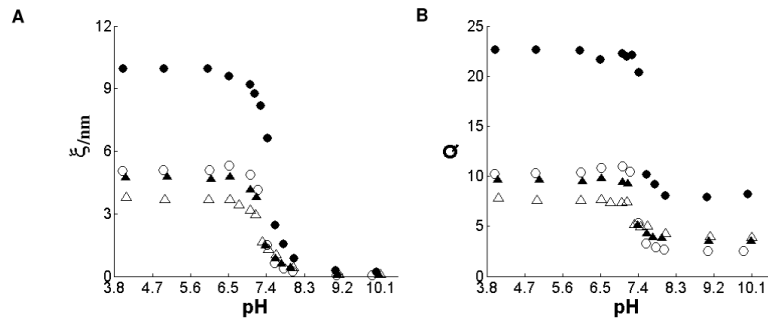


Figure 5. Mesh size (A) and Volume Swelling ratio (B) measurements as a function of pH for formulations with crosslinking ratios of 0.01 (●), 0.025 (○), 0.05 (▲) and 0.10 (△).

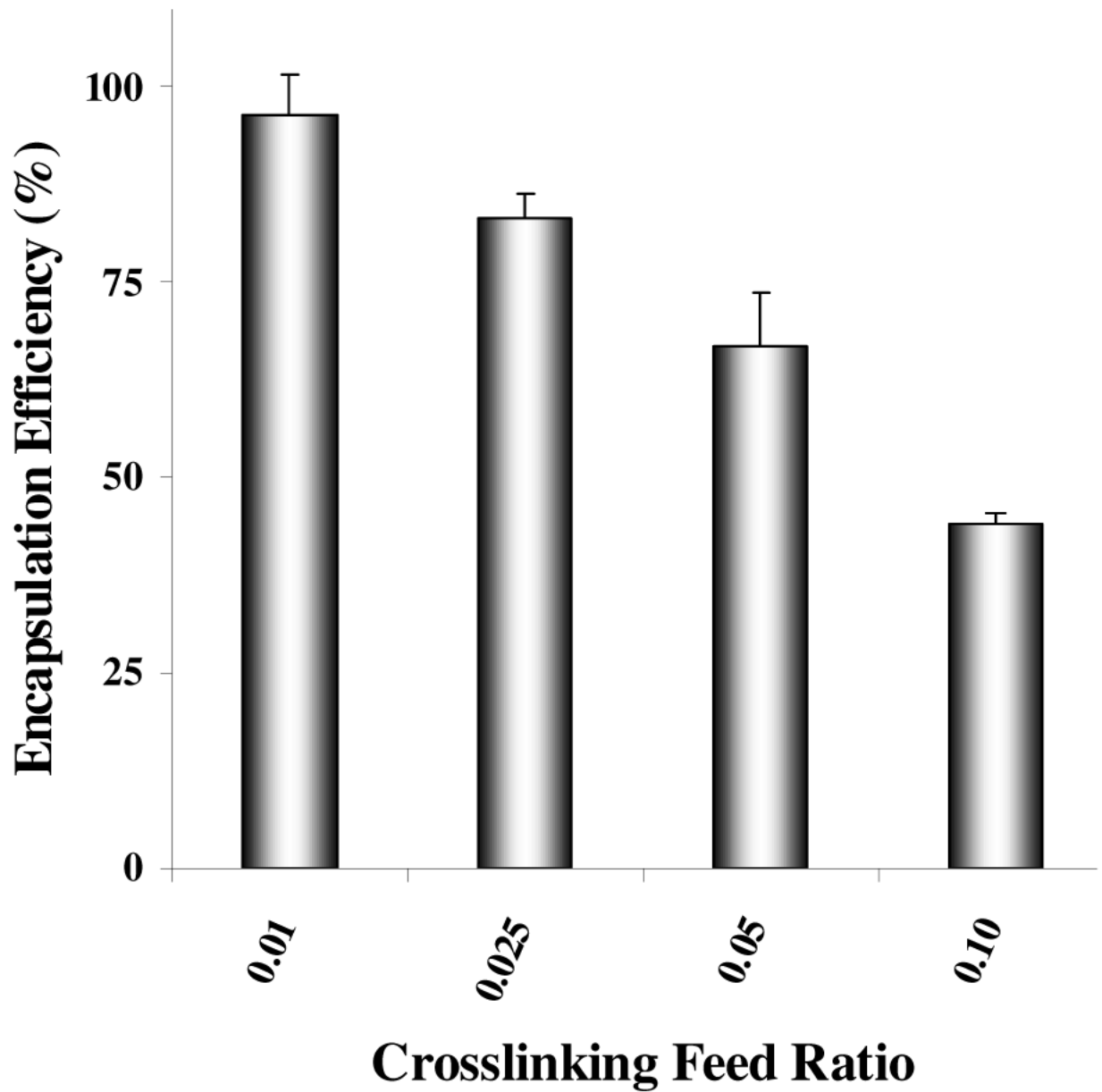


Figure 6. Insulin entrapment efficiency into PDGP nanomatrices at pH 7.4 for different crosslinking densities. Error bars = standard deviation (n=3).

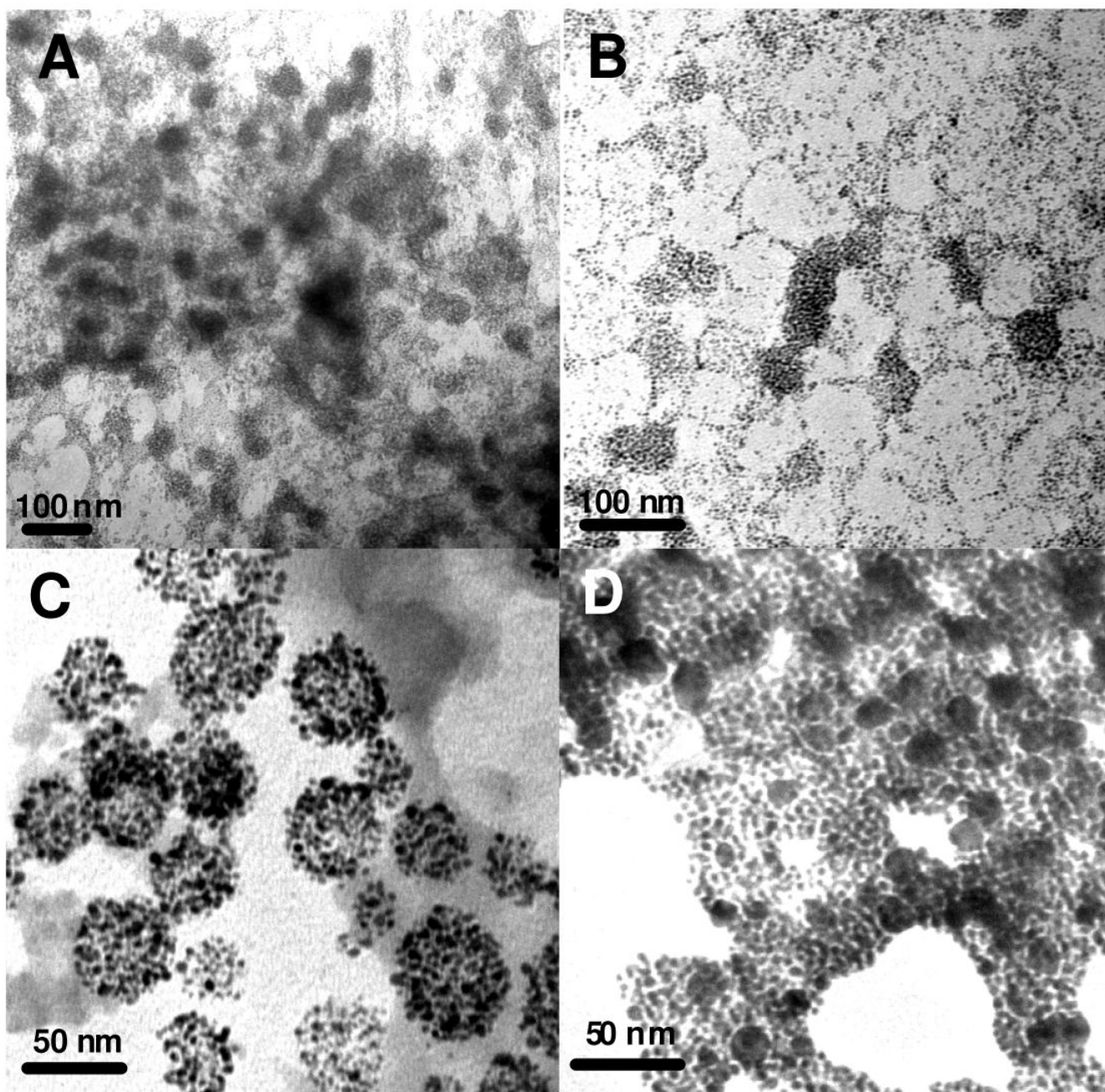


Figure 7. Transmission electron micrographs of colloidal Au loaded into PDGP nanomatrices with crosslinking feed ratios of 0.01 (A), 0.025 (B), 0.05 (C) and 0.10 (D).

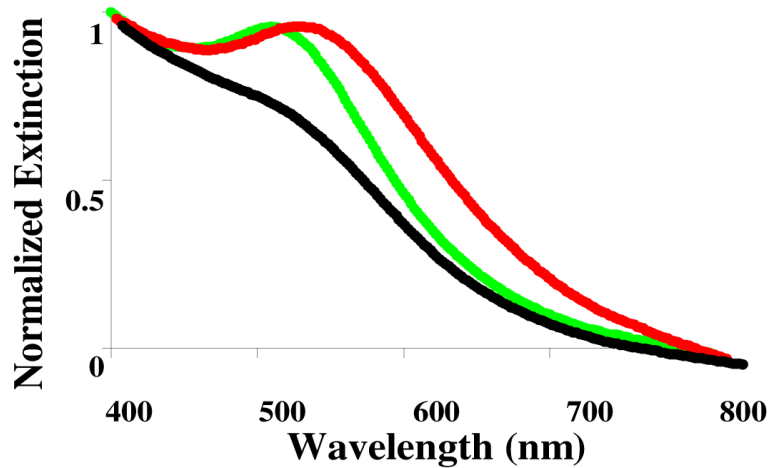


Figure 8. Extinction spectra for Au loaded nanomaterials with 5% (green) and 10% (red) crosslinking and Au colloid alone (black).

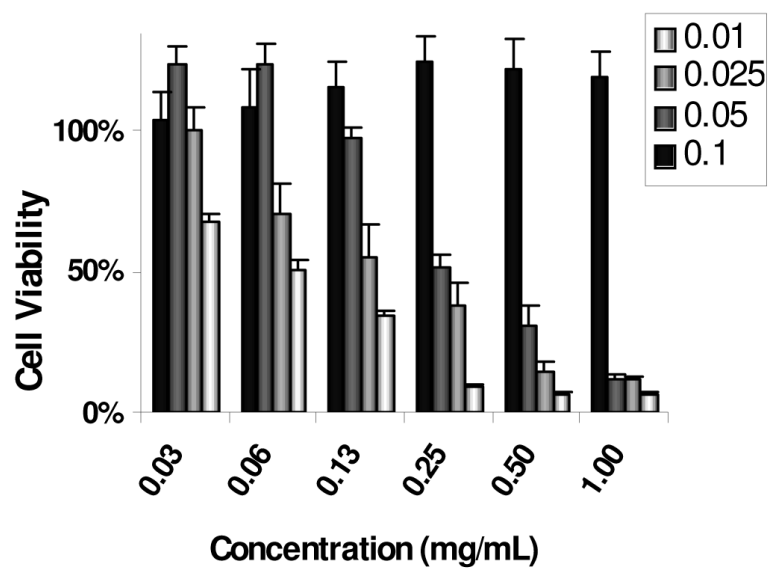


Figure 9. MTS assay of NIH/3T3 fibroblasts exposed to PDGP nanomaterials as a function of concentration and crosslinking density. Each bar represents the mean \pm standard deviation (n=8).

Table 1

Critical swelling pH (pH_{cr}), hydrodynamic diameter (D_H) and ζ -potential in the swollen and collapsed state, and molecular weights between crosslinks (M_c) and mesh sizes (ξ) in the swollen state for different crosslinking mole feed ratios (X)

X	pH_{cr}	D_H (nm) pH=6	D_H (nm) pH=8	ζ (mv) pH=6	ζ (mv) pH=8	M_c	ξ (nm)
0.01	7.60	141 ± 2	99 ± 1	32 ± 4	4.7 ± 3	4414	9.90
0.025	7.59	111 ± 2	68 ± 1	25 ± 5	-1 ± 4	1915	5.04
0.05	7.38	107 ± 1	76 ± 1	20 ± 6	-1 ± 6	1766	4.74
0.10	7.31	99 ± 1	78 ± 1	14 ± 2	-1 ± 2	1302	3.80